Available online at www.sciencedirect.com
SCIENCE DIRECT®
Computational Materials Science 32 (2005) 85–95
COMPUTATIONAL MATERIALS SCIENCE
www.elsevier.com/locate/commatsci

Calculated optical spectra of IV–VI semiconductors PbS, PbSe and PbTe

E.A. Albanesi [a,*], E.L. Peltzer y Blanca [b], A.G. Petukhov [c]

[a] *INTEC-CONICET, Guemes 3450, 3000 Santa Fe, and Facultad de Ingenieria, UNER, 3100 Oro Verde, Argentina*
[b] *IFLYSIB-CONICET and GEMyDE, Facultad de Ingenieria, UNLP, 1900 La Plata, Argentina*
[c] *Physics Department, South Dakota School of Mines and Technology, Rapid City, SD 57701-3995, USA*

Received 7 January 2004; received in revised form 3 April 2004

Abstract

A complete ab initio calculation of the optical properties of the semiconductor compounds PbS, PbSe and PbTe which crystallize in the rock-salt structure, is presented. The electronic structure has been obtained in two approximations for the exchange and correlation potential, the local density approximation and the generalized gradient approximation, comparing the relevant results. Our study includes the spin–orbit interaction. We have calculated the imaginary part of the dielectric function $\varepsilon_2(\omega)$ and the real part $\varepsilon_1(\omega)$ using the Kramers–Kronig relations. In addition, other optical parameters such as the absorption coefficient, the complex refraction index, and the reflectivity are presented. The main features showed by the optical function curves, can be understood on the bases of the band structure of these compounds, and our results can be satisfactory compared with experiments.
© 2004 Elsevier B.V. All rights reserved.

PACS: 71.20.Nr; 78.20.−e; 78.20.Ci
Keywords: Optical properties; Dielectric functions; Linearized augmented-plane-wave method; IV–VI lead salts

1. Introduction

The IV–VI compounds based on the Pb salts, are semiconducting with good grade of polarity, with bondings formed through electrostatic interactions among the ions of the crystal lattice, crystallizing in the rock-salt type structure. Compared for example with the usual III–V compounds, these IV–VI chalcogens present nontypical electronic and transport properties, such as high carrier mobilities, high dielectric constants, narrow band gaps and a positive temperature coefficients [1,2]. These properties make the IV–VI compounds particularly useful as electro-optical devices in the range of 3–30 μm, corresponding to the medium and far infrared. Consequently, many studies and developments have been

* Corresponding author. Tel.: +54 342 4559174; fax: +54 342 4550944.
E-mail address: eaa@intec.ceride.gov.ar (E.A. Albanesi).

0927-0256/$ - see front matter © 2004 Elsevier B.V. All rights reserved.
doi:10.1016/j.commatsci.2004.07.001

undertaken in detecting devices for infrared and visible radiation, laser diodes, and photo-voltaic cells, which are used in many different applications such as medical diagnostic, industrial process monitoring and atmospheric pollution control [3]. Also, quantum confinement devices are evolving with IV–VI materials, particularly PbS, allowing operating devices in optical ranges of technological importance [4]. These factors have motivated the interest in the study of the fundamental behavior of these Pb salt compounds, for which grounded experimental research have been performed on their structural and band properties [1,2,5], electronic structure [6–8] and optical properties [9–14].

There have also been many theoretical studies of the electronic properties of these cubic lead salts, which have been performed with different techniques such as the empirical pseudopotentials, the tight binding method [15–17], the ab initio pseudopotential [18], the orthogonalized-plane-wave (OPW) [19], the Green function method [20], the augmented-plane-wave (APW) [21], and some bulk [22] and optical constants calculated [23] using a mixed k.p-(APW) method. Most of these calculations have been performed within the framework of semiempirical approaches or involving some simplifications such us neglecting the spin–orbit coupling, making the calculation easier and reducing the amount of computing time. The drawback of these calculations is the parameters that need to be fitted to experiments. As a result, the previous methods agree in a general description, but their differences may conduct to different interpretation of the experimental data. So far, and since the description of optical properties with empirical schemes depends upon a correct interpretation of the experimental spectra, first-principles calculations are quite desirable.

There have been previous ab initio calculations on the band structures and electronic properties with the full-potential linearized muffin-tin orbital method [8] and the full-potential linearized augmented-plane-wave (FP-LAPW) [24,25], providing results in good agreement with experiments. In the same line, the aim of this work is to provide a complete ab initio theoretical study of the optical properties of the three salts that Pb forms with S, Se, Te, and a discussion of the fundamentals of the observed spectra.

For our calculations we have used the FP-LAPW method within the density functional theory (DFT), in the form implemented in the WIEN97 code [26]. This is a very accurate first-principles scheme to be used in modeling properties of materials. As part of our treatment, we have used the options of the local density approximation (LDA) for the exchange and correlation potential. This approximation has resulted in a great amount of success in dealing with the calculation of electronic properties, although it failed in describing some important properties, like underestimating the equilibrium lattice constants and the band gaps. A formal correction is obtained when the gradient of the density of electrons is also considered in this functional. This is the so called generalized gradient approximation (GGA) [27,28], which we will use in the formal parameterization scheme of Perdew–Burke–Ernzerhof (PBE) [29]. This corrected functional is semilocal and thus more sensitive to nonspherical components of the density, resulting in a better performance when applied in a full-potential scheme like the WIEN97. The GGA have been applied in a variety of tests, giving great improvements in structural energy differences, and even in describing the correct ferromagnetic ground states of magnetic metals [27,30]. The general gradient approximation can be used for resolving problems requiring better accuracy than the LDA, with only a few more computational requirements than the LDA.

For the quantitative calculation of optical spectra, it is crucial to determine the correct energy band gaps. We will discuss our results on both the LDA and the GGA schemes, together with other usual empirical corrections to the LDA, such as the scissor operator [31], which basically means to adjust the band gap with a constant potential to reproduce the experimental energy band gaps. This last one is often used, particularly in the determination of the band gap offsets [24,32] which appear when considering interfaces between different semiconductors, but also when bulk properties under pressure are studied [33].

There are other calculation schemes for optical properties, which, although they have not been performed on these Pb salts, it is important to mention them as first-principles approaches. The LDA method used in conjunction with a self-

energy operator given as a product of the Green function G times the screened Coulomb interaction W, and called the GW approximation (GWA) of Hedin [34], is often used to obtain well described excited states [35]. However, this one-particle approach produces optical peaks shifted towards higher energies and with intensities that do not reproduce the experimental data well [36]. Arnaud and Alouani [36,37] have developed an all-electron ab initio method within the GWA based on the projector-augmented-wave (PAW) method [38], to study the local-field (LF) and excitonic effects in various types of semiconductors; III–V compounds, Si and C. They showed that the inclusion of local-field effect to the GWA does not change the energy position of the peaks, but reduces considerably the peak intensities of both main peaks, the so called E_1 and E_2, resulting in a better described E_2, but a worsen E_1. By adding the electron–hole interaction, they obtained the oscillator strength shifted towards lower energies, improving the intensity shape of the optical spectra. In Section 2 we will discuss qualitatively how the inclusion of both effects, local-field and excitonic interaction would modify our calculations.

Because of the presence of heavy elements, in our study we have included the spin–orbit interaction. This description splits up some energy bands, and since these are narrow band gap systems the band description are truly improved, particularly in the band gap region where the conformation and symmetry play the main role. Also, these differences are of importance in the optical properties of these materials, since a higher amount and sharp peaks appear.

2. Procedures and discussion of results

For these rock-salt type crystal structures with two atoms per unit cell, we have used in our calculations the experimental values for the lattice parameters [2,6], which are 5.936, 6.124 and 6.462 Å for PbS, PbSe and PbTe, respectively. To allow optimum convergence in the calculation of optical properties, the self-consistent band structure and densities of states (DOS) of the three compounds were calculated in 2024 irreducible k points in the first Brillouin zone (BZ), since spin–orbit interaction was included. We present here the details of PbS along many important directions on the BZ in Fig. 1, with a comparison between both approximations, GGA and LDA, and the DOS in Fig. 2, which were obtained in the GGA approximation. This electronic structure is representative of all cases, and will be used for the discussion purposes on the optical properties for the three lead salts.

In Fig. 1 with the GGA scheme, the deepest band in energy corresponds to a s-like state coming from the anion S, with also a small contribution from the Pb-s state. Fig. 2 shows this band spreading in a narrow energy region of 1.71 eV, with its maximum peak at −11.82 eV. The second band from the bottom that appears, is formed with a main contribution from s-Pb states, with a very low p-Pb component. Also there is a small amount of s and p-like states from the anion S. From Fig. 2 we can see that this band has a width of 2.80 eV, somewhat wider than the previous one, corresponding the maximum at −8.20 eV for s-Pb states. Following through the higher energies, the bands turn to be less well defined due to hybridization. In the L point of the first BZ, and using the double group notation, there is a degenerated L_6^+ band, getting splitted in going across the Λ direction to the Γ point. In other points of the BZ they maintain nondegenerated increasing their dispersion up to 5.01 eV, resulting the proper valence band when reaching the Fermi energy E_F, as shown in Fig. 2. The main contribution to this valence band comes from a strong contribution of the p-S states distributed along the whole band, giving a broad peak at −2.32 eV and a narrow one at about −1.00 eV. Fig. 2 also shows that coincident with the sharp p-S peak, also the s-Pb states makes its maximum contribution. In spite of the fact that the latter is smaller than the former, it becomes very important in the conformation of the band gap, since the little shoulder of these s-Pb states forms the edge of the valence band giving rise to the maximum of the valence band L_6^+. Also, it is observed a contribution from the p-Pb states, which while small, they spread in the whole valence band. At the Γ point, the spin–orbit splitting of the valence bands closer to E_F is of 0.32 eV, while the spin–orbit splitting at the X point

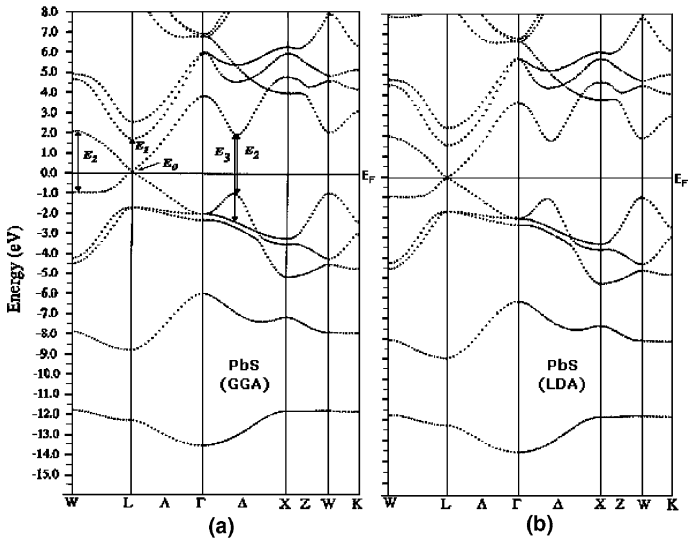

Fig. 1. Calculated energy bands for PbS, including spin–orbit. (a) Using the GGA. The arrows represent possible interband transitions between bands originating the main peaks in the optical function spectra. (b) With the LDA. The general feature results similar to that of the GGA, except for the smaller value of the energy band gap.

results in 0.29 eV. The band gap is direct and appears at the L point. Within the LDA approximation, the general feature are similar to that of GGA, except for the smaller value of the band gap.

In Table 1 we present some electronic-structure parameters comparing them with other calculations since no experimental data are available. Since the general appearance and shape of our calculated bands have very good agreement with reported experimental data [1,8] and other ab initio calculations [8,24], we conclude that our band states are very reliable for the calculation of the optical functions.

The starting point in calculating the optical functions, is a good self-consistent electronic structure. This is a fundamental requisite since the optical functions involve matrix elements from the momentum operator, and the eigenfunctions used in the calculations have to be precise. The inclusion of the spin–orbit interaction is very important to determine the optical properties of this materials, since more peaks appear, and their energies are better established. Because of the importance of the band gap values in the correct characterization of the optical properties, we present them in Table 2, as obtained with the different approaches. It is seen that when LDA is used, they result with the known underestimation, while on the other hand, GGA gives an improvement, providing band gaps in good agreement with experiments in a more formal way than adjusting with the scissor operator the LDA results.

The expression of the imaginary dielectric functions, is computed by Ambroch-Draxl and Abt [39], which for a system with cubic symmetry results in

$$\varepsilon_2 = \frac{4\pi^2 e^2}{m^2\omega^2}\sum_{i,f}\int \mid \langle f \mid p_j \mid i\rangle\mid^2 \times W_i(1-W_f)\delta(E_f - E_i)\,\mathrm{d}^3k \qquad (1)$$

In this expression, $\langle f|p_j|i\rangle$ is the dipole matrix, and f, i, are the final and initial states respectively, W_i is the Fermi distribution function for the ith state, and E_i is the electron's energy in the ith state. Here and in the following expressions, j denotes any of the three components in the Cartesian coordinates. The real part of the dielectric functions is computed from $\varepsilon_2(\omega)$ using the Kramers–Kronig relations in the form

$$\varepsilon_1(\omega)_j = 1 + \frac{2}{\pi}P\int_0^\infty \frac{\omega'\varepsilon_2(\omega')_j}{\omega'^2-\omega^2}\mathrm{d}\omega' \qquad (2)$$

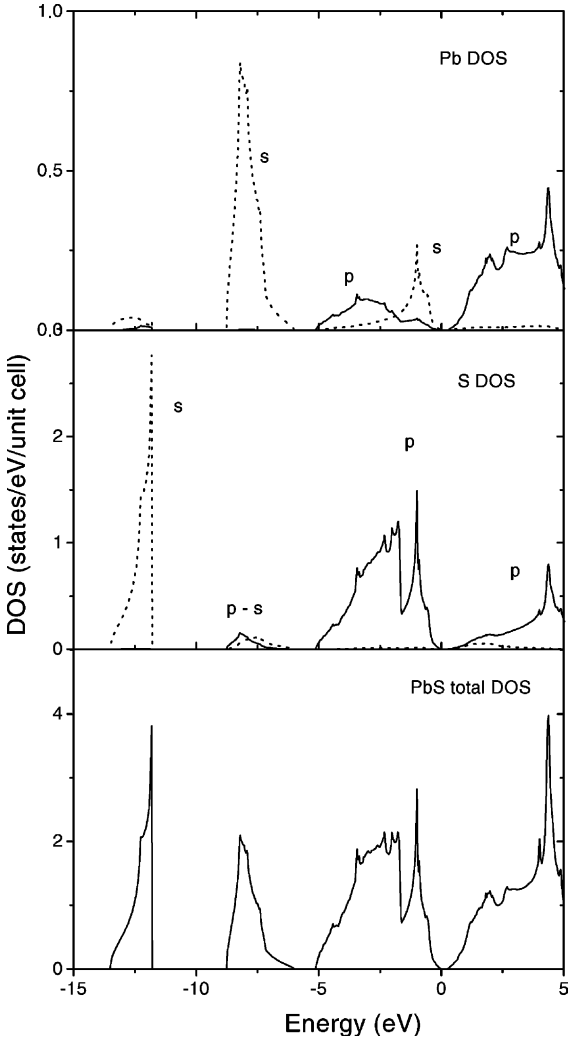

Fig. 2. Density of states, total and by atom, obtained for PbS considering spin–orbit.

where P means the principal value of the integral. The arrows in Fig. 1 represent possible interband transitions giving rise to the main peaks in the optical function curves.

Other important parameters in the optical characterization that we have also calculated, are the optical absorption coefficient, obtained as

$$\alpha(\omega)_j = \frac{2\omega}{c}\left(\frac{-\mathrm{Re}(\varepsilon(\omega)_j) + |\,\varepsilon(\omega)_j\,|}{2}\right)^{1/2} \quad (3)$$

and the complex refraction index $\tilde{n}(\omega)_j = n_R(\omega)_j + ik(\omega)_j$, defined in terms of the refraction index $n_R(\omega)_j$ as its real part, and the extinction coefficient $k(\omega)_j$ as its imaginary part, obtained from $\left(\tilde{n}(\omega)_j\right)^2 = \varepsilon_1(\omega)_j + i\varepsilon_2(\omega)_j$.

Also, we have calculated the reflectivity $R(\omega)_j$ as

$$R(\omega)_j = \left(\frac{1-\tilde{n}(\omega)_j^{\star}}{1+\tilde{n}(\omega)_j^{\star}}\right)^2 \quad (4)$$

We have performed our calculations in the 0–5.5 eV range, in which the experimental measurements take place. In Figs. 3 and 4 we show our calculation for the real part $\varepsilon_1(\omega)$ and for the imaginary part $\varepsilon_2(\omega)$ respectively, of the dielectric function. The imaginary part is related to the energy lost of the incident radiation, and is closely related to the absorption coefficient $\alpha(\omega)$ which appears in Fig. 5. The first energy E_0 corresponds to the step energy of the semiconductor which is about the calculated band gap value, whose assigned transition is $L(5 \rightarrow 6)$. Here the bands are numbered as usual, being the first the lowest band, which for these compounds are the s-like anion bands.

Table 1
Some significant electronic-structure values for PbS, compared with other available calculations

	This work		Other calc.
	LDA	GGA	
$E_g(\Gamma)$	5.68	5.85	5.97[a] 7.14[b]
$E_g(X)$	7.12	7.22	
$\Delta_{s-o}(\Gamma)$	0.34	0.32	
$\Delta_{s-o}(X)$	0.30	0.29	

Values are in eV.
[a] Ref. [24].
[b] Ref. [33].

Table 2
Summary of calculated and experimental band gaps, considering spin–orbit coupling

	This work		Expt.[a]
	LDA	GGA	
PbS	0.037	0.176	0.286
PbSe	0.012	0.121	0.165
PbTe	0.028	0.160	0.190

Values are in eV.
[a] Ref. [2,6].

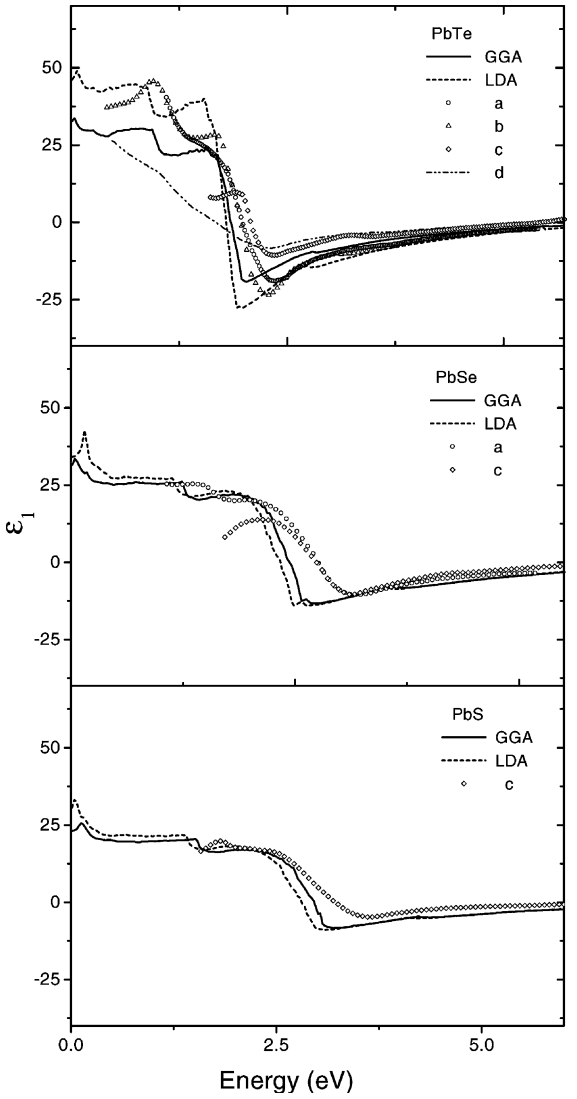

Fig. 3. The GGA and the LDA calculations of the real part $\varepsilon_1(\omega)$ of the dielectric function, compared with the experimental data (a) Refs. [12,13], (b) Ref. [14], (c) Ref. [11] and (d) Ref. [9].

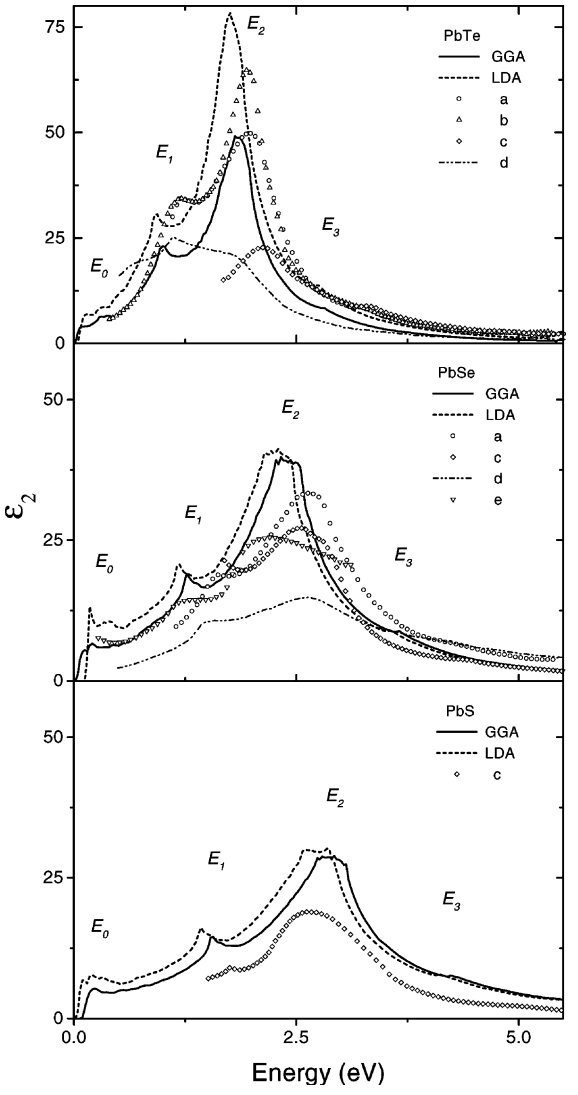

Fig. 4. The GGA and the LDA calculations of the imaginary part $\varepsilon_2(\omega)$ of the dielectric function, compared with the experimental data (a) Refs. [12,13], (b) Ref. [14], (c) Ref. [11], (d) Ref. [9] and (e) Ref. [40].

Within the GGA scheme, the E_0 peak appears with the values of 0.231, 0.122 and 0.150 eV respectively for PbS, PbSe and PbTe compounds. The E_1 peak next is located at 1.57 eV (PbS), 1.27 eV (PbSe), and 1.01 eV (PbTe), it is the first shoulder that appears in the spectrum, which is originated in the transitions $\Sigma(5 \rightarrow 6)$ (Σ is the direction between Γ and K in the BZ which does not appear in Fig. 1) and $L(5 \rightarrow 7)$, formed by transitions between s-Pb valence states and p-Pb and a few of p-anion conduction states. Our values are in close agreement with the experimental values assigned to this peak (Table 3). The absorption coefficient $\alpha(\omega)$ plotted in Fig. 5 shows an increased value corresponding to the energy E_1, a correct indication that at the transition energies the absorption of the materials is increased. The $\varepsilon_2(\omega)$ spectrum

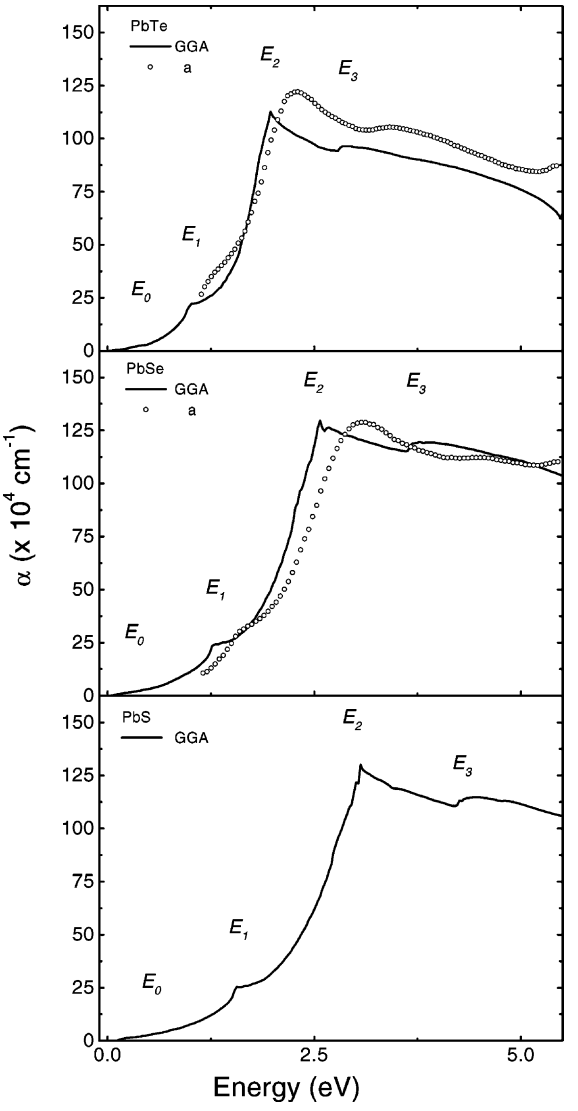

Fig. 5. Calculated absorption coefficient $\alpha(\omega)$ as a function of energy, compared with existing experimental data (a) Refs. [12,13].

keeps increasing until the main peak E_2 is formed, it is called the reflectivity peak for which the maximum magnitude in the ε_2 curve is obtained. For PbS and PbSe, it is a flat peak with some dispersion with possible energies between 2.73 and 3.06 eV for PbS, and 2.27 and 2.54 eV for PbSe. For PbTe it results in a sharper peak at 1.80–1.86 eV. The absorption coefficient $\alpha(\omega)$ grows strongly and monotonically between E_1 and E_2 having a maximum and sharp peak at this later energy. The contributions to the E_2 peak come from the interband transitions in the direction $\Sigma(5 \rightarrow 7)$ and $\Delta(5 \rightarrow 6)$, corresponding to interband transitions between p-anion (some from s-Pb) valence states and p-Pb and p-anion conduction states. After the E_2 peak, the calculated values of $\varepsilon_2(\omega)$ decrease in energy, and then the small E_3 peak appears at the energy of 4.23, 3.66, and 2.82 eV, for PbS, PbSe and PbTe respectively, which is originated in the interband transitions $\Delta(4 \rightarrow 6)$ and in some amount on $\Sigma(4 \rightarrow 7)$ between p-anion valence states and p-Pb and p-anion conduction states. The absorption coefficient decreases smoothly between E_2 and E_3, presenting a small peak at this last energy, decreasing again after it.

In Figs. 3–5 we have compared our calculated functions with the available experimental data. For the dielectric functions $\varepsilon_1(\omega)$ and $\varepsilon_2(\omega)$, there are many different techniques giving appreciable differences in the energy where the peaks are

Table 3
A comparison between our calculated values with GGA and experimental data, for the characteristic energy peaks E_0, E_1, E_2, E_3 appearing in the optical function spectra

System	Peak	This work	Expts.
PbS	E_0	0.231	0.286[a]
	E_1	1.57	1.83–2.15[b]
	E_2	2.73–3.06	3.0–3.67[c]
	E_3	4.23	5.08–5.27[d]
PbSe	E_0	0.122	0.165[a]
	E_1	1.27	1.59–2.18[e]
	E_2	2.27–2.54	2.65–3.12[f]
	E_3	3.66	4.10–5.3[g]
PbTe	E_0	0.150	0.190[a]
	E_1	1.01	1.08–1.60[h]
	E_2	1.80–1.86	1.98–2.30[i]
	E_3	2.82	3.25–3.5[j]

Values are in eV.
[a] Refs. [2,6].
[b] Refs. [9–11].
[c] Refs. [9–11].
[d] Refs. [9,11].
[e] Refs. [9,11,13].
[f] Refs. [9,13].
[g] Refs. [9,11,13].
[h] Refs. [10,12].
[i] Refs. [9,11,12]
[j] Refs. [9–12].

Table 4
Calculated dielectric constants $\varepsilon_1(0)$ with GGA, compared with experiments

System	This work	Expts.
PbS	23.12	
PbSe	31.50	
PbTe	32.78	37.09[a]
		26.34[b]

[a] Ref. [14].
[b] Ref. [9].

positioned, but more significant in the intensities of the peaks. The E_2 intensity is one important feature of the spectrum, since it can give a measure of the cleanliness of a surface, particularly when spectroscopic ellipsometry is used [12,13]. This advantageous technique permits direct measurement of the real and imaginary parts of the dielectric function $\varepsilon(\omega)$, and is less affected by fluctuations or by the sample conditions, than for example, direct reflectance and transmition [9] measurements that deal with power measurements. Our calculations with GGA compare better with the experimental data measured by Suzuki et al. [12,13] using spectroscopic ellipsometry. As a general rule, GGA tends to a small underestimation of the peak energy positions, and follows acceptably the intensities shape and balance between E_1 and E_2 peaks. We believe that if spectroscopic ellipsometry experiments were performed on PbS, our GGA calculations would adjust them very well in energy positions and intensities. In Figs. 3 and 4 we present for comparison also our LDA calculation, which show the expected underestimation. The main difference however is obtained for PbTe, where the intensity of the E_2 peak is very overestimated. This behavior is related to the fact that there is a broadening in the optical spectra when the anion is lighter, produced by an increasing dispersion between bands when going from Te to S in the band structure calculations. The experimental values for these peaks are in Table 3. The inclusion of LF and electron–hole interaction would improve LDA description of the intensities for $\varepsilon_2(\omega)$ for the three compounds, although the underestimation of the energy positions would persists. The same situation would be valid for PbSe and PbS with GGA scheme, although for PbTe a decrease in the function intensities would not be desirable.

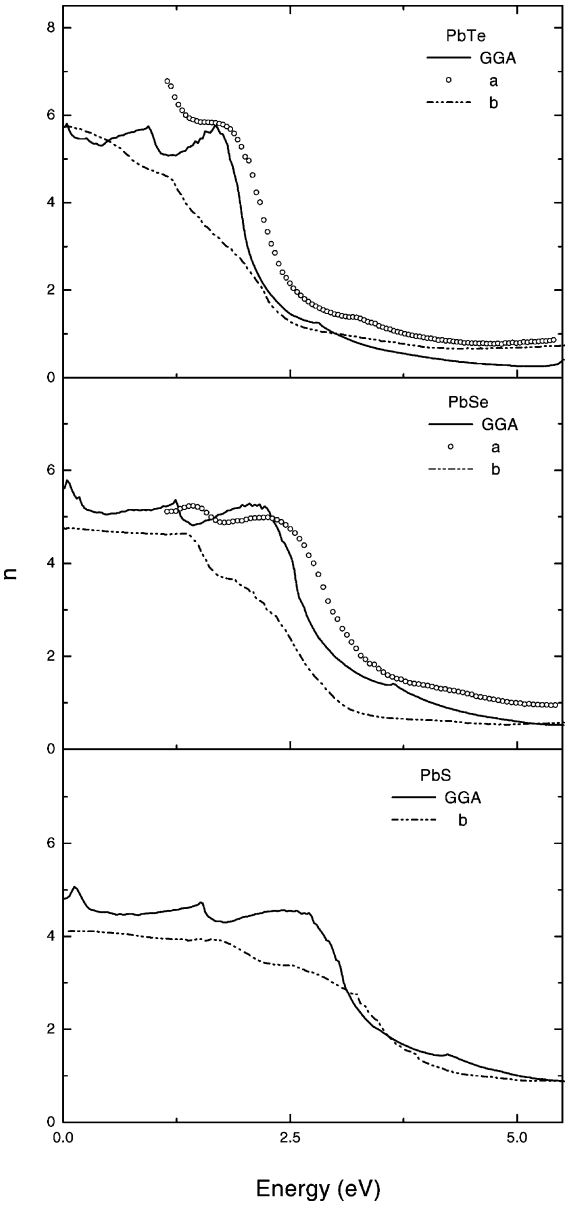

Fig. 6. Calculated spectral variation of the real part $n_R(\omega)$ of the complex refraction index, compared with experimental data (a) Refs. [12,13] and (b) Ref. [9].

The real part of the dielectric constant $\varepsilon_1(\omega)$ (Fig. 3), gives the dispersive behavior of these compounds. It results in a broad shoulder followed by

the strong decrease in the region of energies corresponding to the maximum absorption peak E_2, where the functions become negative, increasing slowly after it toward zero at higher energies. For the real dielectric function, the most important quantity is the zero frequency limit $\varepsilon_1(0)$, since it gives the static dielectric constant in the zero frequency limit, which we have shown in Table 4. Even when LDA gives some overestimation, mainly for PbTe, our GGA calculations coincide

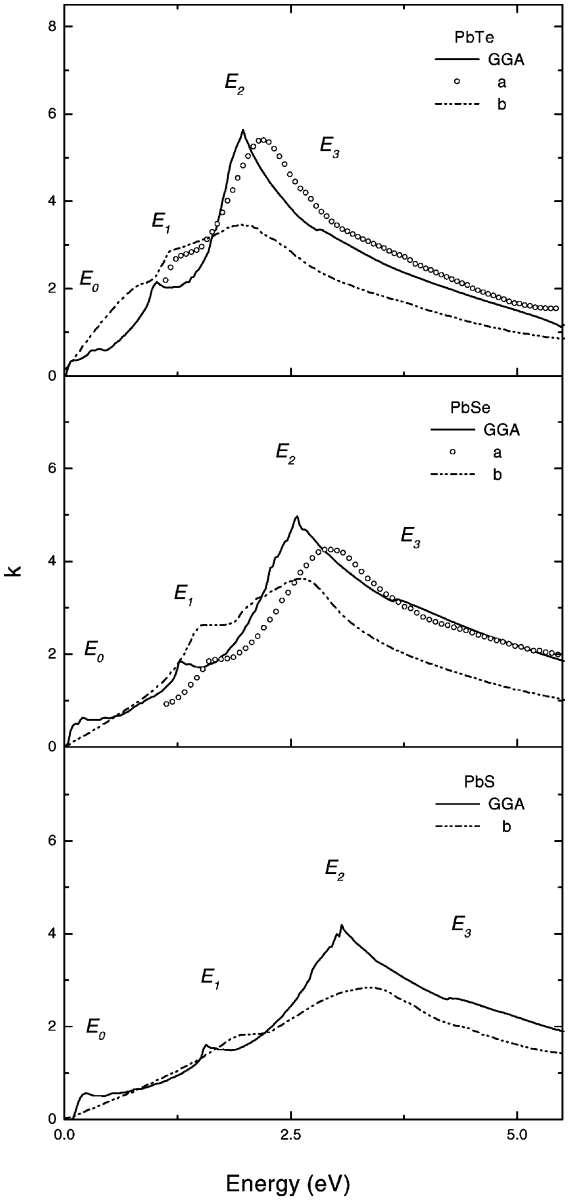

Fig. 7. Calculated spectral variation of the imaginary part $k(\omega)$ of the complex refraction index, compared with existing experimental data (a) Refs. [12,13] and (b) Ref. [9].

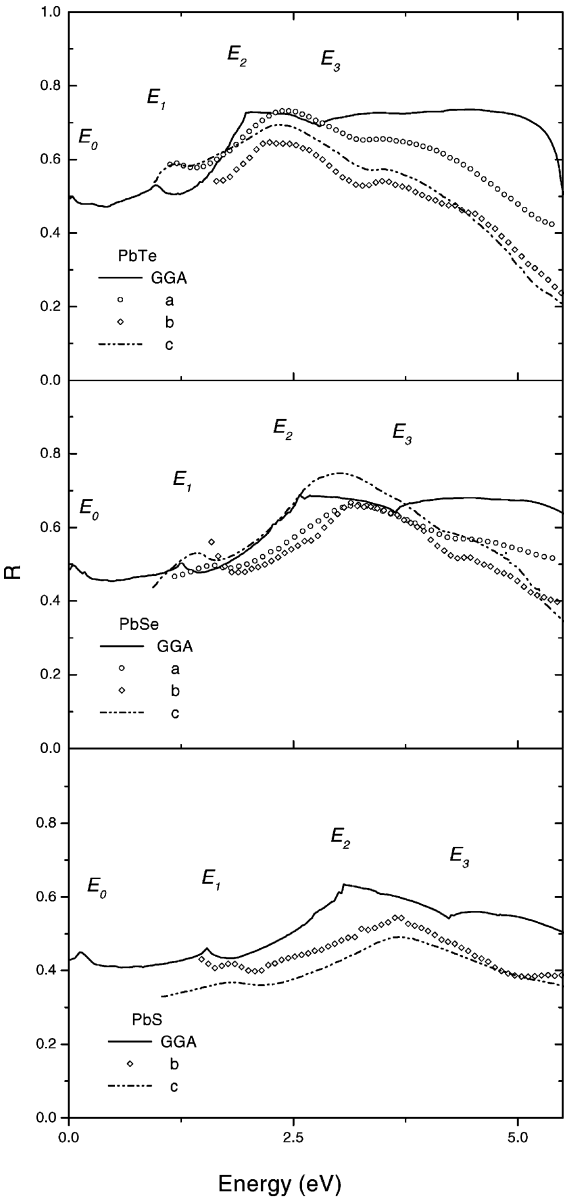

Fig. 8. Calculated spectral variation of the reflectivity coefficient $R(\omega)$ compared with experimental data (a) Refs. [12,13], (b) Ref. [11] and (c) Ref. [9].

very well with the available experimental data, even for PbS and PbSe for which the data finish far before from the $\omega = 0$ condition. The expected lowering that LF effect would produce, could be compensated by the rising effect of the electron–hole interaction [36] if both were considered, giving no significant changes in our results.

Figs. 6 and 7 show our results for the complex refractive index $\tilde{n}(\omega)$, in which the imaginary part $k(\omega)$ shows an absorptive behavior, with peaks at energies E_0 through E_3, while the real part $n_R(\omega)$ which represents the usual refraction index has the dispersive form of a step, presenting a broad shoulder with the main steep descend at E_2. It also presents small steep descend at the other relative maxima E_0, E_1, E_3 in $k(\omega)$. The reflectivity coefficient $R(\omega)$ is presented in Fig. 8, and it results according to the discussion on $\varepsilon_2(\omega)$ and $\alpha(\omega)$, presenting local minima at about the local maxima of the absorption curve $\alpha(\omega)$. The maxima calculated reflectivity is approximately of 64%, 69%, and 73% for PbS, PbSe and PbTe respectively, for radiation higher than about E_2 energy. The general features of our calculated curves for the complex refractive index $\tilde{n}(\omega)$ (Figs. 6 and 7) and for the reflectivity coefficient $R(\omega)$ (Fig. 8) are in good agreement with the experimental curves presented in Refs. [12,13], even when GGA maintains a small underestimation of the peak energy positions.

3. Conclusions

We have presented a complete first-principles study of the optical functions of the three more important cubic lead salts PbS, PbSe and PbTe. In our calculations we have used the FP-LAPW method in the GGA and the LDA schemes. The study has included the spin–orbit effects which results of fundamental importance in giving adequated band structures and optical calculations. While the LDA provides acceptable results in the general features of the calculated optical functions, it underestimates the energy band gap, resulting that the characteristic optical interband transitions occur at lower values than the experimental peaks. A way to overcome this could be by correcting the calculated band gaps with the scissor operator, to fit the experimental energies. Our calculations in the GGA, give practically the same improvement without the need of any empirical correction. Also, we have explained the origin of the main contributions and the behavior of the optical functions, and our results can be satisfactorily compared to existing experimental studies, even though some dispersion exists among the experimental results obtained by measuring with different techniques. Our GGA calculations of the static dielectric constants is very satisfactory, while the LDA gives some overestimation, mainly for PbTe. We have also qualitatively discussed the effects that the inclusion of the local-field and the electron–hole interaction would produce in our results. We believe that these effects could be worth testing through formal calculations, considering the existing differences between III–V materials and these IV–VI Pb-compounds.

Acknowledgments

The authors acknowledge financial support from the Consejo Nacional de Investigaciones Científicas y Técnicas (CONICET), and the Universidad Nacional de Entre Ríos (UNER), Argentina.

References

[1] G. Nimtz, B. Schlicht, B. Dornhaus, Narrow Gap Semiconductors: Springer Tracts in Modern Physics, Spinger, New York, 1983, and references therein.
[2] R. Dalven, in: H. Ehrenreich, F. Seitz, D. Turnbull (Eds.), Solid State Physics, vol. 28, Academic Press, New York, 1973, p. 179.
[3] Z. Feit, M. McDonald, R.J. Woods, V. Archambauld, P. Mak, Appl. Phys. Lett. 66 (1996) 738.
[4] A. Lipovskii, E. Kolovkova, V. Petricov, I. Kang, A. Olkhovets, T. Krauss, M. Thomas, J. Silcox, F. Wise, Q. Shen, S. Kycla, Appl. Phys. Lett. 71 (1997) 3406.
[5] A. Miller, G. Saunders, Y. Yogurtcu, J. Phys. C 14 (1981) 1569.
[6] M.L. Cohen, J.R. Chelikowsky, Electronic Structure and Optical Properties of Semiconductors, second ed. Springer Series in Solid State Sciences, vol. 75, Springer-Verlag, Berlin, 1989.
[7] T. Grandke, L. Levy, M. Cardona, Phys. Rev. B 18 (1978) 3847.

[8] V. Hinkel, H. Hoak, C. Mariana, L. Sorba, K. Horn, N.E. Christensen, Phys. Rev. B 40 (1989) 5549.
[9] M. Cardona, D.L. Greenaway, Phys. Rev. 133 (1964) A1685.
[10] D.E. Aspnes, M. Cardona, Phys. Rev. 173 (1968) 714.
[11] S.E. Kohn, P.Y. Yu, Y. Petroff, Y.R. Shen, Y. Tsang, M.L. Cohen, Phys. Rev. B 8 (1973) 1477.
[12] N. Suzuki, S. Adachi, Jpn. J. Appl. Phys. 33 (1994) 193.
[13] N. Suzuki, K. Sawai, S. Adachi, J. Appl. Phys. 77 (1995) 1249.
[14] D. Korn, R. Braunstein, Phys. Rev. B 5 (1972) 4837.
[15] P.J. Lin, L. Kleinman, Phys. Rev. 142 (1966) 478.
[16] G. Martinez, M. Schlüter, M.L. Cohen, Phys. Rev. B 11 (1975) 651.
[17] J.A. Valdivia, G.E. Barberis, J. Phys. Chem. Solids 56 (1995) 1141.
[18] K. Rabe, J. Joannopoulos, Phys. Rev. B 32 (1985) 2302.
[19] F. Herman, R.L. Kortum, I. Ortenburger, J.P. Van Dike, J. Phys. 29 (Suppl.) (1968) C4-62.
[20] H. Overhoff, U. Rössler, Phys. Stat. Sol. 37 (1970) 691.
[21] J.H. Conklin Jr., L.E. Johnson, G.W. Pratt, Phys. Rev. 137 (1965) A1282.
[22] L.G. Ferreira, Phys. Rev. 167 (1965) 801.
[23] D.D. Buss, N.J. Parada, Phys. Rev. B 1 (1970) 2692.
[24] S. Wey, A. Zunger, Phys. Rev. B 55 (1977) 13605.
[25] E.A. Albanesi, E.C. Okoye, C.O. Rodriguez, E.L. Peltzer y Blanca, A.G. Petukhov, Phys. Rev. B 61 (2000) 16589.
[26] P. Blaha, K. Schwarz, J. Luitz, Viena University of Technology, 1997 (Improved and updated version of the WIEN code, published by P. Blaha, K. Schwarz, P. Sorantin, S.B. Rickey, Comp. Phys. Commun. 59 (1990) 399).
[27] J.P. Perdew, J.A. Chevary, S.H. Vosko, K.A. Jackson, M.R. Pederson, D.J. Sing, C. Fiolhais, Phys. Rev. B 46 (1992) 6671.
[28] J.P. Perdew, Y. Wang, Phys. Rev. B 45 (1992) 13244.
[29] J.P. Perdew, K. Burke, M. Ernzerhof, Phys. Rev. Lett. 77 (1996) 3865;
J.P. Perdew, K. Burke, M. Ernzerhof, Phys. Rev. Lett. 78 (1997) 1396.
[30] J.P. Perdew, S. Kurth, A. Zupan, P. Blaha, Phys. Rev. B 82 (1999) 2544.
[31] M. Lanoo, M. Schlüter, L.J. Sham, Phys. Rev. B 32 (1984) 3890.
[32] E.A. Albanesi, W.L. Lambrecht, B. Segall, J. Vac. Sci. Tech. B 12 (1994) 2470.
[33] Z. Nabi, B. Abbar, S. Mecabih, A. Khalfi, N. Amrane, Comput. Mat. Sci. 18 (2000) 127.
[34] L. Hedin, Phys. Rev. 139 (1965) A796;
L. Hedin, S. Lundquist, in: H. Ehrenreich, F. Seitz, D. Turnbull (Eds.), Solid State Physics, vol. 23, Academic Press, New York, 1969, p. 1.
[35] F. Araysetianwan, G. Gunnarson, Rep. Prog. Phys. 61 (1998) 237.
[36] B. Arnaud, M. Alouani, Phys. Rev. B 63 (2001) 085208.
[37] B. Arnaud, M. Alouani, Phys. Rev. B 62 (2000) 4464.
[38] P.E. Blöchl, Phys. Rev. B 50 (1994) 17953.
[39] C. Ambroch-Draxl, R. Abt, authors of the code extension for optical properties, The calculation of optical properties within WIEN97, ICTP Lecture Notes, 1998, unpublished.
[40] T.S. Moss, Optical Properties of Semiconductors, Butterworth, London, 1959, p. 189.